Tools to Characterize the Correlated Nature of Collective Dynamics

R. Vilela Mendes
CMAFcIO, Universidade de Lisboa
Faculdade de Ciências C6, 1749-016, Lisboa, Portugal
rvilela.mendes@gmail.com
rvmendes@fc.ul.pt
label2.tecnico.ulisboa.pt/vilela

Carlos Aguirre
GNB, Escuela Politécnica Superior
Universidad Autonoma de Madrid, Campus de Cantoblanco
Ctra de Colmenar Km 16, 28049 Madrid, Spain

Synchronization, which occurs for both chaotic and nonchaotic systems, is a striking phenomenon with many practical implications for natural phenomena and technological applications. However, even before synchronization, strong correlations and complex patterns occur in the collective dynamics of natural systems. To characterize their nature is essential for understanding many phenomena in physical and social sciences as well as the perspectives to control their behavior. Because simple correlation measures are unable to characterize these collective patterns, we have developed more general methods for their detection and parametrization. The emergence of patterns of strong correlations before synchronization is illustrated in a few models. They are shown to be associated with the behavior of ergodic parameters. The models are then used as a testing ground of the new pattern characterization tools.

Keywords: correlation; synchronization; chaotic dynamics; complex patterns

1. Introduction

When natural systems are made to interact with one another, collective properties emerge that would be hard to predict from their individual properties. Synchronization [1–8] is a most striking cooperative phenomenon in nature that has been shown to be of fundamental importance in fields as diverse as the operation of heart pacemaker cells [9, 10], circadian cycles [11], epileptic seizures [12, 13], schizophrenia disorders [14, 15], neuronal firing [16–18], animal behavior [19], social fads, the integration of cognitive tasks

https://doi.org/10.25088/ComplexSystems.30.1.1

[20–22], synchronization-based computation [23] and even quantum systems [24].

Many natural systems can be described as networks of oscillators coupled to each other. Coupled oscillators may display synchronized behavior, that is, follow a common dynamical evolution. Synchronization properties are dependent on the coupling pattern among the oscillators, represented as an interaction network [25–33]. The central question here concerns the emergence of coherent behavior: synchronization or other types of correlation. This occurs for systems with regular behavior as well as for systems that have chaotic dynamics (lasers, neural networks, physiological processes, etc.). Chaotic systems are characterized by a strong sensitivity to initial conditions, and two identical uncoupled chaotic systems will become uncorrelated after a long time even if they start from very similar (but not identical) states. Nevertheless, the coupling of such systems can make them follow the same chaotic trajectories [34–39]. The degree of synchronization is usually measured by a parameter related to the coherence of the phases or by the entropy of the phase distribution [40]. Most of the work developed so far in this field has emphasized criteria for synchronizability and the relation between network structure and the emergence of synchronized behavior. Typically, the emphasis has been on the distinction between synchronized and incoherent behavior or on their coexistence, as in the so-called chimera states [41–46]. Some exploration, mostly numerical, has also been done on partially synchronized states, clustering, dimensional reduction and so on [47–54].

Striking as it is, synchronization is not the whole story because, without or before synchronization, much subtler correlations occur in the global dynamical behavior of interacting systems. However, whereas synchronization or partial (cluster) synchronization is easy to detect, it is not so clear how to detect and quantify other types of correlations. Little has been done on the way of developing effective tools to characterize, in a quantitative manner, the striking correlation phenomena that may appear before synchronization or even in the apparently incoherent phases of some systems. That is the main purpose of this paper.

As a first step and to illustrate the fact that, even at very small interaction strength, a system of N previously independent systems becomes enslaved to a collective, essentially one-dimensional dynamic, a deformed Kuramoto model is studied in Section 2. In some limit of this model, a rigorous calculation of the Lyapunov spectrum is possible, and we are able to reveal the nature of the strong correlations that are present even very far away from the synchronization threshold. In addition, the model provides a good hint about the relevance of the ergodic parameters to the collective behavior. Having

also found in this section that a simple correlation measure is unable to properly characterize the dynamics, we proceed to develop in Section 3 some new tools for this purpose. One is based on the geometrical characterization of the dynamics, another is related to dynamical clustering using spectral methods and another is based on a version of the notion of conditional Lyapunov exponents. Admittedly, the new tools are more complex than simple correlations. Nevertheless, they are not hard to program and even implement as an automatic diagnostic.

Then, in Section 4, application of the tools is illustrated in the deformed Kuramoto model, on a model of coupled oscillators with a triangle interaction and on an integrate-and-fire model. The first two models have essentially the same dynamical complexity as the Kuramoto model, widely used as a paradigm for synchronizing systems, and are representative of the stylized behavior found in many collective systems in biology, population dynamics, socioeconomic phenomena, and others. The third model relates to neuroscience. For clarity, most of the numerical illustrations of the results are presented for a small (~100) number of interacting agents; however, in all cases, to exclude finite size effects, simulations with much larger numbers were performed with qualitatively similar results.

2. The Deformed Kuramoto Model: An Illustration of the Emergence of Strong Correlations before Synchronization

The main model used in the past for the study of synchronization phenomena was the Kuramoto model [55],

$$\frac{d\theta_i}{dt} = \omega_i + \frac{K}{N-1}\sum_{j=1}^{N}\sin\left(\theta_j - \theta_i\right). \tag{1}$$

The analysis of the Kuramoto model has a long history, with a number of important results obtained throughout the years [56, 57], but a full understanding of its dynamics is still lacking, and most of the rigorous results are only strictly valid in the thermodynamic limit.

Here we use a model of the same type. This model, first mentioned in [58], is

$$x_i\left(t+1\right) = x_i(t) + \omega_i + \frac{K}{N-1}\sum_{j=1}^{N}\pi f^{(n)}\left(x_j - x_i\right) \pmod{\pi}, \tag{2}$$

with $x_i \in [-\pi, \pi)$ and $f^{(n)}$ a deformed version of the Kuramoto interaction

$$f^{(n)}(x) = \operatorname{sign}(x)\left(\sin\left(\frac{|x|^n}{\pi^{n-1}}\right)\right)^{1/n}. \tag{3}$$

https://doi.org/10.25088/ComplexSystems.30.1.1

For $n = 1$, $f^{(1)} = \sin(x)$ and when $n \to \infty$, it becomes (Figure 1)

$$f^{(\infty)}(x_j - x_i) = \frac{1}{\pi}(x_j - x_i) \pmod 1. \tag{4}$$

For the numerical examples, the ω_i will follow a Cauchy distribution

$$p(\omega) = \frac{\gamma}{\pi\left[\gamma^2 + (\omega - \omega_0)^2\right]}. \tag{5}$$

The $f^{(\infty)}$ interaction will be used to derive parameters that characterize the correlations that emerge before synchronization. However, they can also be easily computed in more general systems.

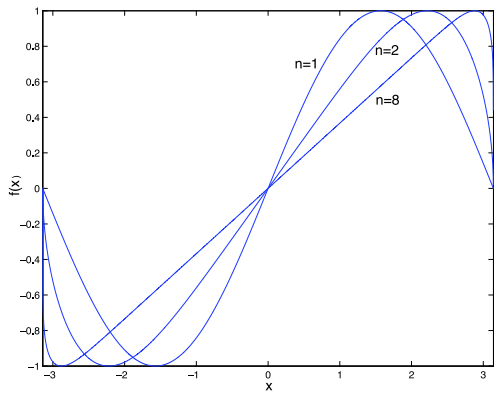

Figure 1. The $f^{(n)}$ interaction function.

For coupled dynamical systems, an order parameter for synchronization is, for example [4],

$$R_n(t) = \left| \sum_{m=1}^{N} A_{n,m} e^{ix_m(t)} \right|, \tag{6}$$

where A is the adjacency matrix. For the fully coupled system we consider, it is simply

$$r(t) = \left| \frac{1}{N} \sum_{j=1}^{N} e^{ix_j(t)} \right|. \tag{7}$$

In Figures 2, 3 and 4 we display the results of numerical simulation of the system in equation (2) with $f^{(\infty)}$, $N = 100$, $K = 0.2$, $K = 0.4$ and $K = 0.8$. A typical distribution of the Cauchy-distributed frequencies ω_i is plotted in Figure 5. We start from random initial conditions and plot the color-coded coordinates $x_i(t)$ from $t = 500$ to $t = 600$. It can be seen that for the small K, the coordinates seem to be mostly

uncorrelated, whereas for larger K, a large degree of synchronization is observed. This is also the information that is obtained from the behavior of the order parameter $r(t)$.

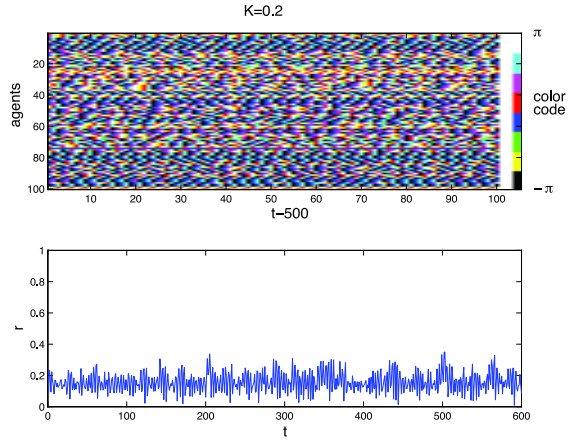

Figure 2. Coordinates x_i and order parameter $r(t)$ for $K = 0.2$.

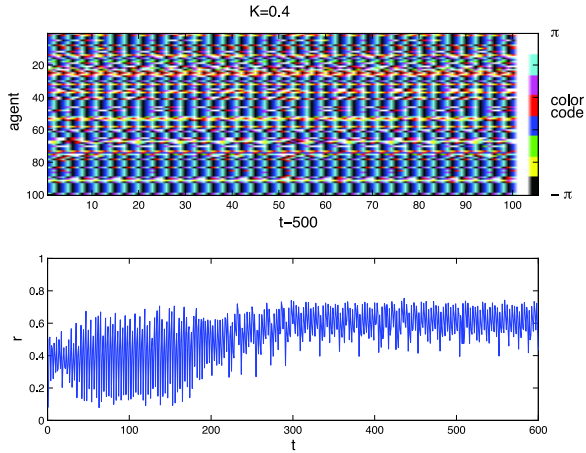

Figure 3. Coordinates x_i and order parameter $r(t)$ for $K = 0.4$.

The behavior of the model is similar to Kuramoto's. An important question is whether synchronization is all there is in the dynamics of interacting oscillators. In the past, several authors have found, for example, synchronized cluster formation before the full synchronization transition. The simplicity of the present model allows for further exploration of this question and a useful hint is, as usual, obtained

from the computation of the ergodic parameters [59]. In particular, the Lyapunov spectrum of the model (equation (2)) in the $n \to \infty$ case may be obtained exactly.

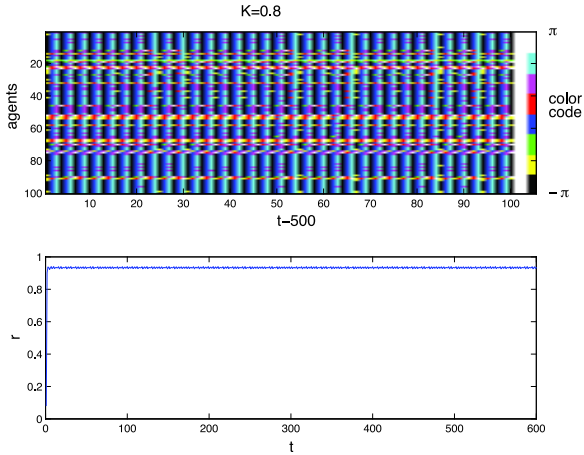

Figure 4. Coordinates x_i and order parameter $r(t)$ for $K = 0.8$.

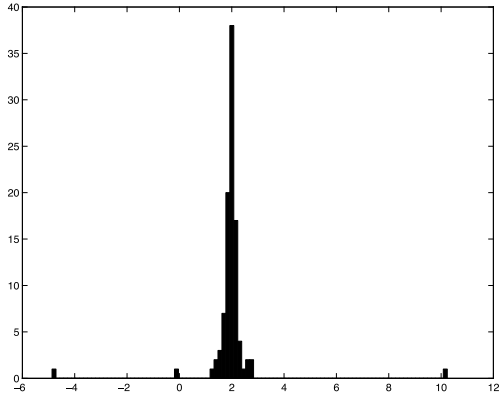

Figure 5. A typical distribution of the Cauchy-distributed frequencies ω_i.

When $K = 0$, there are N neutral directions; that is, the effective dynamical dimension is N and the Lyapunov spectrum contains N zeros. However, as soon as $K > 0$, the Lyapunov spectrum consists of one isolated zero and $\log\left(1 - NK \big/ \left(N - 1\right)\right)$, $(N - 1)$ times. Therefore, although it is only for sufficiently large K that synchronization effects seem to occur, there are, for any small $K > 0$, $N - 1$ contracting directions. The effective dynamical dimension is one for any small $K > 0$.

As soon as there is a (positive) interaction between the units, they are, in the ergodic sense, enslaved to a single collective dynamic. Notice that this is not a pathology of this model. Numerical simulation of the Kuramoto and other models also shows a drastic reduction of the effective dimension long before the synchronization transition.

The fact that the Lyapunov spectrum of the deformed Kuramoto model in the $n \to \infty$ limit may be obtained exactly provides important information about the mechanisms that occur before and at synchronization. The eigenvectors of the Jacobian are

$$\begin{pmatrix} 1 \\ 1 \\ 1 \\ \vdots \\ \vdots \\ 1 \end{pmatrix}; \begin{pmatrix} 1 \\ -1 \\ 0 \\ \vdots \\ \vdots \\ 0 \end{pmatrix}; \begin{pmatrix} 1 \\ 1 \\ -2 \\ 0 \\ \vdots \\ 0 \end{pmatrix}; \cdots; \begin{pmatrix} 1 \\ 1 \\ 1 \\ 1 \\ \vdots \\ -N+1 \end{pmatrix},$$

the first one being associated with the eigenvalue 1 and all the others with $\left(1 - NK \big/ (N-1)\right)$. Denoting by x_i the agents' coordinates, the eigenmodes associated with these eigenvectors are

$$Y_{N,p} = \sum_{i=n}^{n+p-1} x_i - p x_{n+p}.$$

For $K \neq 0$ and before synchronization, these modes follow complex periodic orbits that converge to fixed points when synchronization sets in. Therefore, two distinct phenomena are found here. The first is the dimension reduction at $K = 0$ and then the convergence to fixed points of the eigenmotions associated with the negative Lyapunov exponents. Here the dimension reduction threshold is quite sharp at $K = 0$, but in other models it is more gradual.

The synchronization order parameter (equation (7)) cannot by itself describe the strong correlations and dimensional reduction that occur before synchronization. As shown for the simple model (equation (2)) in the $n \to \infty$ limit, characterization of the correlations may be obtained by the projections on the eigenvectors of the Lyapunov matrix. However, our aim is to develop general methods that might be applied to any system when there is no access to its solutions or even to the equations that generate the time series.

3. Characterizing Correlations: The Tools

Will a correlation measure be sufficient to unravel all the complexities that arise before synchronization? To explore this possibility, we have computed the correlation of the agent dynamics for the deformed

Kuramoto model. That is, we have computed the increments of the coordinates (on the circle) for a long time interval, and from them the matrix of correlations. A typical example is shown in Figure 6 with the same color code as Figure 2 for positive correlation and black for zero or negative correlation.

In Figure 6, many different correlations of several intensities can be seen at $K = 0.2$. However, it is not clear from examination of this figure how to characterize the nature of the correlations nor how they evolve as the synchronization regime is approached. This has led us to propose several other methods, which were then tested on several models. The aim is, as stated before, to characterize the nature of the correlations that occur before synchronization or even in systems that never synchronize. One method is based on the geometrical characterization of the dynamics, another is related to dynamical clustering using spectral methods and another is based on a version of the notion of conditional Lyapunov exponents.

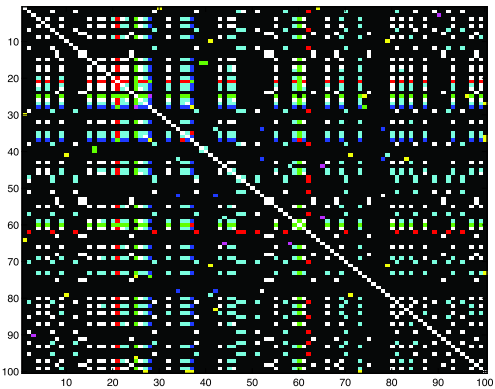

Figure 6. The agents' correlation matrix for the deformed Kuramoto model when $n \to \infty$ and $K = 0.2$.

3.1 The Geometry of the Dynamics

Given a set of N time series, a distance between each pair of series can be defined. One possibility is to consider the Euclidean distance

$$d_{ij} = \frac{1}{T - t_0} \sqrt{\sum_{t=t_0}^{T} \left(x_i(t) - x_j(t)\right)^2} \ . \tag{8}$$

Then, using the technique of multidimensional scaling (MDS), embed the N time series as points in a Euclidean space. MDS begins with an $N \times N$ distance matrix $D = \{d_{ij}\}$, and the aim is to find a configuration of points in a p-dimensional space such that the coordinates of the points yield a Euclidean distance matrix with elements that are as

close as possible to the distances in the original distance matrix (but not exactly the same if the original distances are not Euclidean).

We proceed as follows: denote by Y the matrix of coordinates in the embedding p-dimensional Euclidean space

$$Y = \begin{pmatrix} y_{11} & y_{12} & \cdots & \cdots & y_{1p} \\ y_{21} & y_{22} & \cdots & \cdots & y_{2p} \\ \vdots & \vdots & \vdots & \vdots & \vdots \\ y_{N1} & y_{N2} & \cdots & \cdots & y_{Np} \end{pmatrix} \tag{9}$$

and consider the following decomposition of the squared distance matrix

$$d_{ij}^2 = \left|\overrightarrow{y_i} - \overrightarrow{y_j}\right|^2 = b_{ii} + b_{jj} - 2b_{ij}. \tag{10}$$

Then, the elements of the $N \times N$ matrix B,

$$B = YY^T, \tag{11}$$

are recovered from

$$b_{ij} = -\frac{1}{2}\left\{d_{ij}^2 - \frac{1}{n}\left(\sum_{j=1}^{n} d_{ij}^2 + \sum_{i=1}^{n} d_{ij}^2 - \frac{1}{n}\sum_{i,j=1}^{n} d_{ij}^2\right)\right\}, \tag{12}$$

where by a translation of the origin in R^p we make $\sum_{i=1}^{N} y_{ik} = 0$ for all k.

We diagonalize the matrix B reconstructed by equation (12),

$$B = \mathrm{V}\Lambda V^T, \tag{13}$$

with $\Lambda = (\lambda_1 \cdots \lambda_n)$ $(\lambda_1 \geq \lambda_2 \geq \cdots \geq \lambda_N)$ being the diagonal matrix of eigenvalues and $V = [V_1, \ldots, V_N]$ the matrix of normalized eigenvectors. Whenever the dimension p of the embedding space is smaller than N, the rank of B is p (with the last $N - p$ eigenvalues being zero). We may write

$$B = V^* \Lambda^* V^{*T}, \tag{14}$$

where V^* contains the first p eigenvectors and Λ^* the first p eigenvalues. Then a solution for Y is $Y = V^* \Lambda^{*1/2}$.

When the input distance matrix is not Euclidean, the matrix B is not positive definite. In such a case, some of the eigenvalues of B will be negative and correspondingly, some coordinate values will be complex numbers. If B has only a small number of small negative eigenvalues, it is still possible to use the eigenvectors associated with the p largest positive eigenvalues.

For the time series case, after the Euclidean embedding of the orbits is done, we obtain a cloud of points (a point for each orbit).

https://doi.org/10.25088/ComplexSystems.30.1.1

The shape and effective dimension of the cloud are obtained by reducing the coordinates to the center of mass and computing the inertial tensor

$$T_{ij} = \sum_{k=1}^{N} y_i(k) y_j(k). \tag{15}$$

Let $\lambda(T)$ be the eigenvalues of T. Once the eigenvalues $\{\lambda_k\}$ and eigenvectors $\{V_k\}$ of T are found, the relevant quantities, to characterize the correlations, are the projections (x_i, V_k) of the coordinate vectors on the eigenvectors, in particular on those associated with the largest eigenvalues.

3.2 Dynamical Clustering

Here we want to develop a tool to detect the dynamical communities that emerge from the interaction. For this purpose, the relevant quantities characterizing the dynamics of each agent are the coordinate increments

$$\Delta_i(t) = x_i(t) - x_i(t-1), \tag{16}$$

which may be used to find a dynamical distance of the agents

$$d_{ij} = \sqrt{\sum_{t=1}^{T} \left|\Delta_i(t) - \Delta_j(t)\right|^2}\ . \tag{17}$$

From the distances, define an adjacency matrix

$$A_{ij} = \exp\left(-\beta\left(d_{ij} - d_{\min}\right)\right), \tag{18}$$

a degree matrix

$$(G)_{ii} = \sum_{j \neq i} A_{ij} \tag{19}$$

and a Laplacian matrix

$$L = G - A. \tag{20}$$

The lowest eigenvalues in the L-spectrum provide information about the dynamical communities insofar as they minimize the RatioCut of K communities [60],

$$\text{RatioCut}(C_1, \ldots, C_K) = \frac{1}{2} \sum_{k=1}^{K} \frac{W\left(C_k, \overline{C_k}\right)}{\left|C_k\right|}, \tag{21}$$

with $W\left(C_k, \overline{C_k}\right) = \sum_{i \in C_k, j \in \overline{C_k}} A_{ij}$ being the sum of the external connections of the community C_k, and $\left|C_k\right|$ the number of elements in the C_k community.

3.3 The Conditional Lyapunov Spectrum

An issue of some relevance in multi-agent systems is to compare the view that each agent has of its dependence on the dynamics of the other agents with the actual dependence on the dynamics of the whole network. This is captured by the notion of *conditional exponents*. Conditional exponents, first introduced by Pecora and Carroll [35] in their study of synchronization of chaotic systems, have been shown to be good ergodic invariants [61], playing an important role as self-organization parameters [62]. The conditional exponents are computed in a way similar to the Lyapunov exponents but with each agent taking into account only its neighbors, not the whole system. However, for the time average required for the calculation of the ergodic parameters, the actual global dynamic is used.

For a system with the neighborhood degree characterized by the adjacency matrix, the calculation of the conditional exponents spectrum is equivalent to the computation of the Jacobian of a modified dynamic where the interaction is weighed by the proximity of the agents (i.e., by the adjacency matrix). Nevertheless, the Jacobian is averaged over the orbits of the actual dynamics. For example, for the interacting oscillators of the deformed Kuramoto model, the Jacobian would be computed for a fictitious dynamic,

$$x_i(t+1) = x_i(t) + \omega_i + \frac{K}{N-1}\sum_{j=1}^{N} A_{ij}\pi f^{(n)}(x_j - x_i). \tag{22}$$

The integrated difference of the conditional and the Lyapunov spectrum is an important parameter to characterize the correlated dynamics.

Another promising technique to characterize the correlations occurring before synchronization has been developed by Lopez and Rodriguez [40] who, by considering the Hilbert transform of the coupled time series, obtain an evolving phase and then compute the entropy of the phase distribution. We will not deal here with this technique and refer to [40] for details.

How the techniques discussed do indeed provide information on the correlations of the collective dynamics will be clear by their application to a few models in the next section.

4. Illustration of the Tools on Some Models

In this section, the characterization tools described before are applied to the deformed Kuramoto model, to a model of coupled oscillators with a triangle interaction and to an integrate-and-fire model. The first two models have essentially the same dynamical complexity as

https://doi.org/10.25088/ComplexSystems.30.1.1

the original Kuramoto model, widely used as a paradigm for synchronizing systems, and are representative of the stylized behavior found in many collective systems in biology, population dynamics, socioeconomic phenomena and others. The third model relates to the neuron dynamics models used in neuroscience.

4.1 The Deformed Kuramoto Model

4.1.1 The Geometry of the Dynamics

We have applied the geometrical technique to equation (2), the distance of agent i to agent j being the sum of the distances on the circle of the last 100 time steps. Embedding each 100-times orbit as a point in Euclidean space and using MDS, the eigenvalues $\lambda(B)$ of the B matrix were obtained.

The coordinates of the embedded dynamics are then reduced to the center of mass and the inertial tensor is computed,

$$T_{ij} = \sum_{k=1}^{N} y_i(k) y_j(k), \tag{23}$$

the eigenvalues $\{\lambda_k(T)\}$ being the eigenvalues of T and $\{V_k\}$ its eigenvectors.

Figures 7 and 12 show the results of the geometrical analysis for the dynamics of the model (equation (2)). Figures 7, 9 and 11 show the eigenvalues of the B and T matrices and Figures 8, 10 and 12 the projection of the dynamics on the first and second eigenvectors of T. Of particular interest is the fast reduction in the geometrical dimension of the dynamics, as measured by the fast convergence to zero of

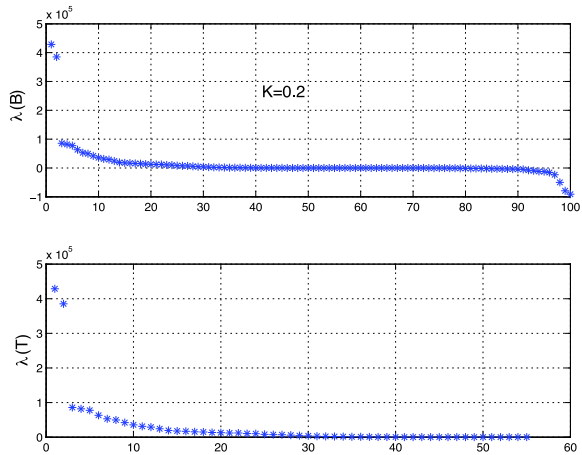

Figure 7. Eigenvalues of the B (equation (11)) and T (equation (15)) matrices for $K = 0.2$.

the $\lambda(T)$ eigenvalues for $K \neq 0$. The whole dynamic seems to be approximately embedded in a two-dimensional subspace. Therefore, the projections on the first two (dominant) eigenvectors, which display very distinct organized patterns, exhibit the strong correlations that already exist before synchronization sets in.

The projection of the embedded coordinates $\{x_i\}$ on the eigenvectors V_k associated with the largest eigenvalues of T may be considered as the new order parameters that characterize the correlations that occur before synchronization. Also of interest are the parameters $P_k = \sum_{i=1}^{N} |(x_i, V_k)|$.

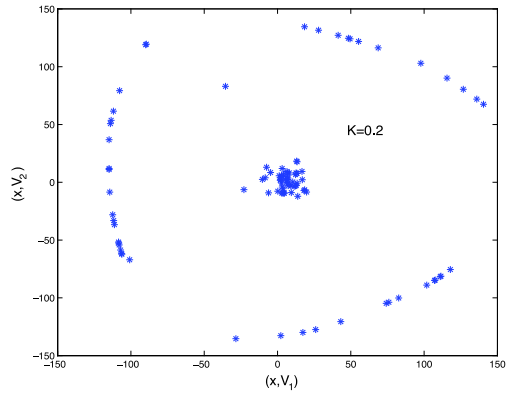

Figure 8. Projection of the dynamics on the first and second eigenvectors for $K = 0.2$.

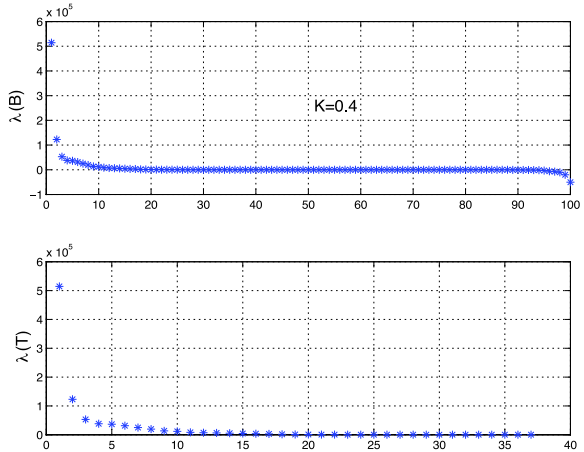

Figure 9. Eigenvalues of the B (equation (11)) and T (equation (15)) matrices for $K = 0.4$.

https://doi.org/10.25088/ComplexSystems.30.1.1

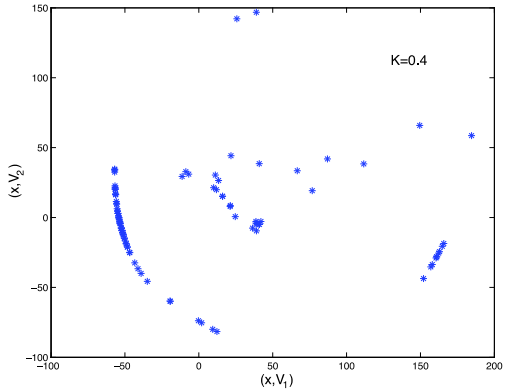

Figure 10. Projection of the dynamics on the first and second eigenvectors for $K = 0.4$.

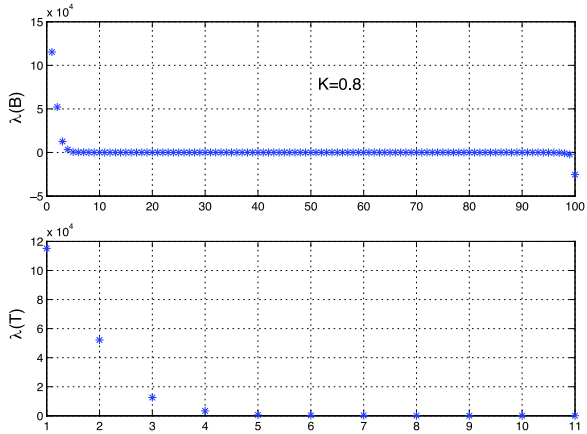

Figure 11. Eigenvalues of the B (equation (11)) and T (equation (15)) matrices for $K = 0.8$.

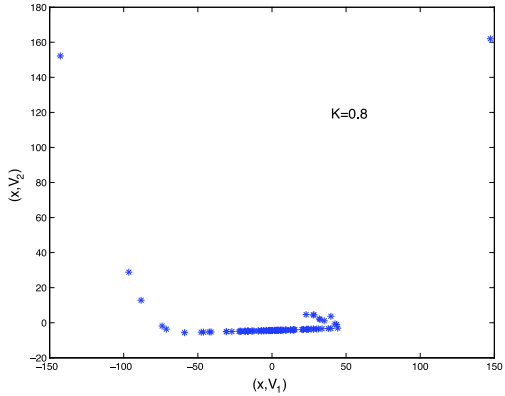

Figure 12. Projection of the dynamics on the first and second eigenvectors for $K = 0.8$.

4.1.2 Dynamical Clustering

Distances and adjacency matrices were computed from the coordinate increments (equations (16) to (19)). In Figures 13 to 15, we have plotted the spectrum of the Laplacian matrix L, as well as the structure of the second and third eigenvectors, to show the nature of the dominant communities.

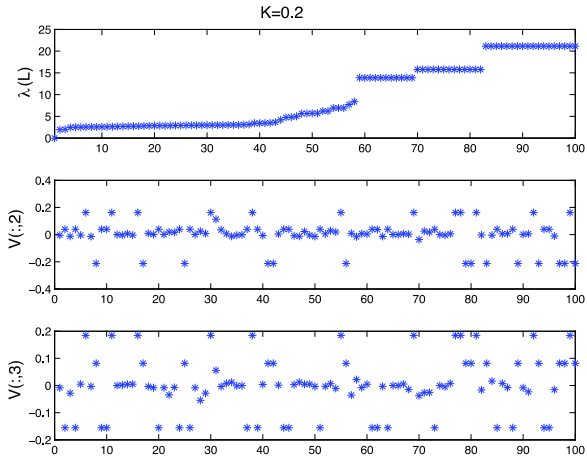

Figure 13. The spectrum of the Laplacian matrix L and the second and third eigenvectors ($K = 0.2$).

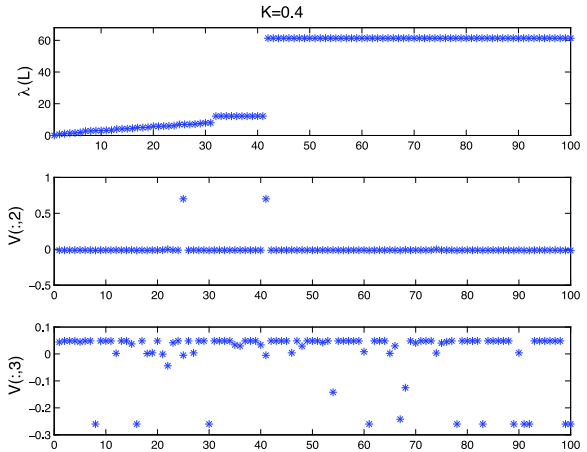

Figure 14. The spectrum of the Laplacian matrix L and the second and third eigenvectors ($K = 0.4$).

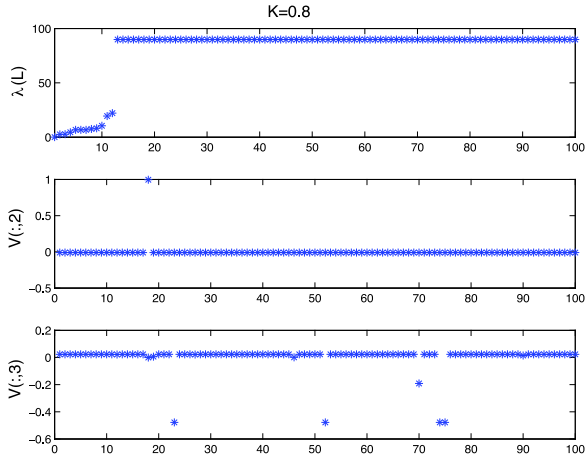

Figure 15. The spectrum of the Laplacian matrix L and the second and third eigenvectors ($K = 0.8$).

4.1.3 The Conditional Exponents Spectrum

As explained before, the conditional exponents are obtained from the Jacobian weighed by the agent's proximity (i.e., by the adjacency matrix) averaged over the orbits of the actual dynamics. For the deformed Kuramoto model, the Jacobian is computed for a fictitious dynamic

$$x_i(t+1) = x_i(t) + \omega_i + \frac{K}{N-1}\sum_{j=1}^{N} A_{ij}\, \pi f^{(n)}(x_j - x_i). \tag{24}$$

The adjacency matrix that is used is the same that was derived in Section 4.1.2.

In Figures 16 to 18, the spectrum of the Lyapunov number $(\mu_i = e^{\lambda_i})$ of the system (equation (2)) is compared with the conditional number $\left(\mu_i^C = e^{\lambda_i^C}\right)$ spectrum for $K = 0.2$, 0.4 and 0.8.

It can be seen that for a small coupling, the conditional number spectrum is still close to the spectrum of the uncoupled system, meaning that the "perception" of the agents is very close to a situation where their dynamics looks like free dynamics, although in fact it is already fully correlated, as evidenced by the Lyapunov spectrum. As the coupling increases, the conditional number spectrum becomes closer and closer to the Lyapunov spectrum. The integrated difference of the two spectra is an important parameter to characterize the correlated dynamics.

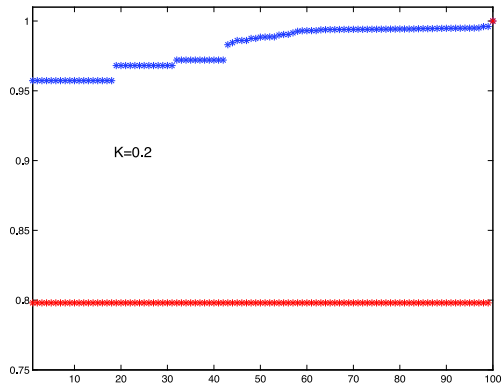

Figure 16. Conditional (blue) versus Lyapunov (red) numbers ($K = 0.2$).

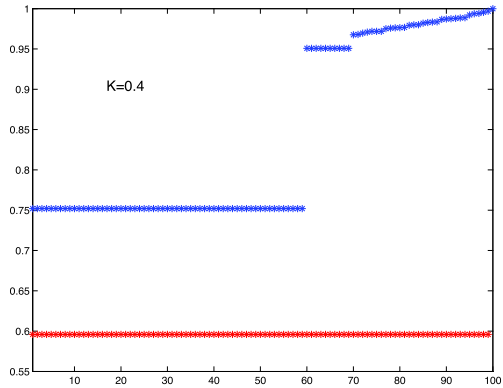

Figure 17. Conditional (blue) versus Lyapunov (red) numbers ($K = 0.4$).

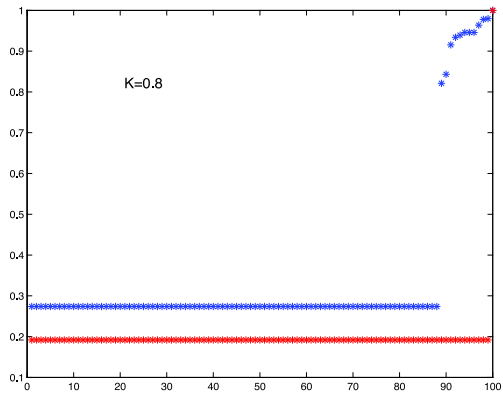

Figure 18. Conditional (blue) versus Lyapunov (red) numbers ($K = 0.8$).

https://doi.org/10.25088/ComplexSystems.30.1.1

4.2 Coupled Oscillators with a Triangle Interaction

Here the dynamical law is

$$x_i(t+1) = x_i(t) + \omega_i + \frac{K}{N-1}\sum_{j=1}^{N} g(x_j - x_i) \pmod{\pi}, \tag{25}$$

$g(x)$ being the function displayed in Figure 19. The frequencies ω_i are also assumed to follow a Cauchy distribution.

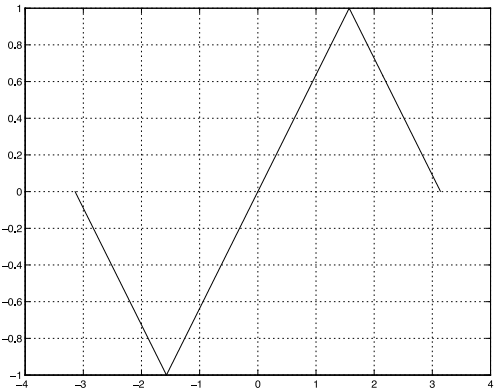

Figure 19. The "triangle" function.

As in the previous example, for small values of the coupling (K), the order parameter r fluctuates around small values, whereas for large values the synchronization is apparent (Figures 20 to 22).

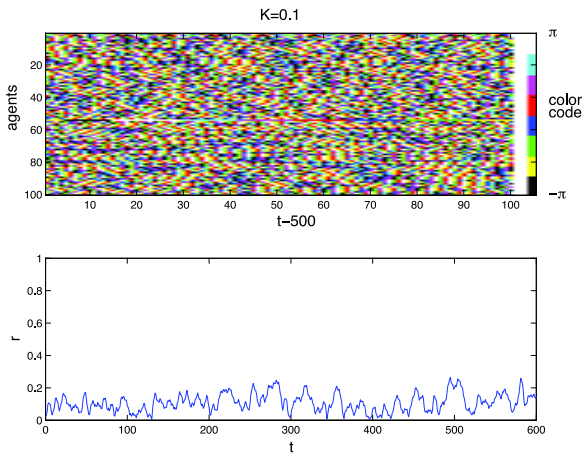

Figure 20. Coordinates x_i and order parameter $r(t)$ for $K = 0.1$ (triangle interaction).

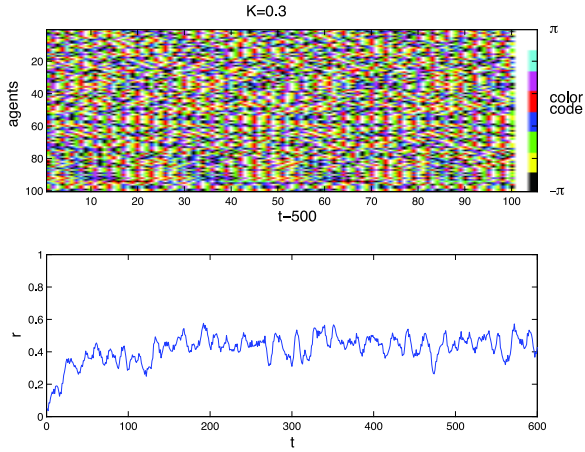

Figure 21. Coordinates x_i and order parameter $r(t)$ for $K = 0.3$ (triangle interaction).

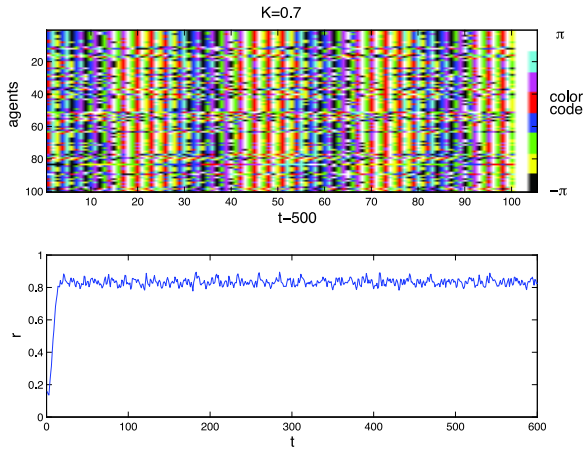

Figure 22. Coordinates x_i and order parameter $r(t)$ for $K = 0.7$ (triangle interaction).

However, by computing numerically the Lyapunov spectrum (Figure 23), we see that already for very small K values, instead of N neutral directions there are a number of contracting directions, implying a reduction in the effective dimension. This is not apparent from the behavior of the order parameter r, emphasizing once more the need to characterize the correlations that appear before synchronization.

https://doi.org/10.25088/ComplexSystems.30.1.1

For the triangle interaction, the dynamical dimension reduction is not as dramatic as in the deformed Kuramoto model, as is evident from the behavior of its Lyapunov spectrum (Figure 23). Therefore, we expect the correlations to develop at a slower pace as the coupling (K) increases.

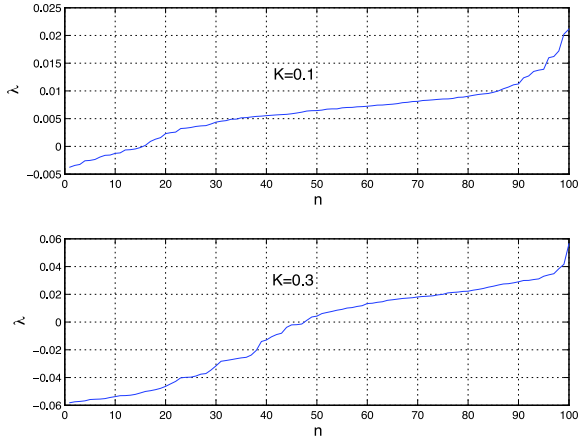

Figure 23. Numerically computed Lyapunov spectrum for the triangle interaction at $K = 0.1$ and $K = 0.3$.

4.2.1 The Geometry of the Dynamics

In the absence of interaction ($K = 0$), the inertial tensor has many large eigenvalues and the projections of the orbits on the two largest eigenvectors show no distinctive pattern (Figure 24).

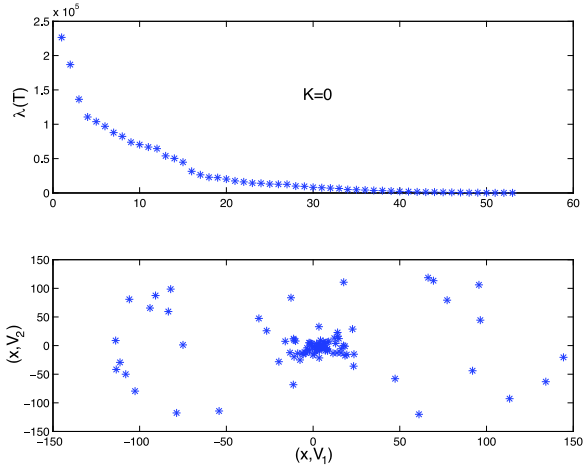

Figure 24. Eigenvalues of the matrix T and projection of the dynamics on the first and second eigenvectors for $K = 0$ (triangle interaction).

It can be seen that the case $K = 0.1$ (Figures 25 and 26) is not very different from the $K = 0$ case, showing that strong correlations have not yet developed.

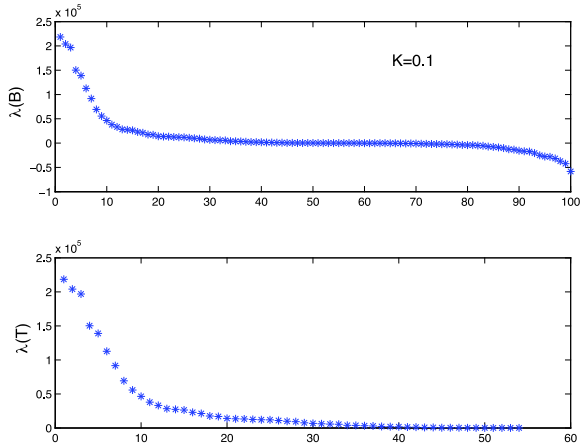

Figure 25. Eigenvalues of the B and T matrices for $K = 0.1$ (triangle interaction).

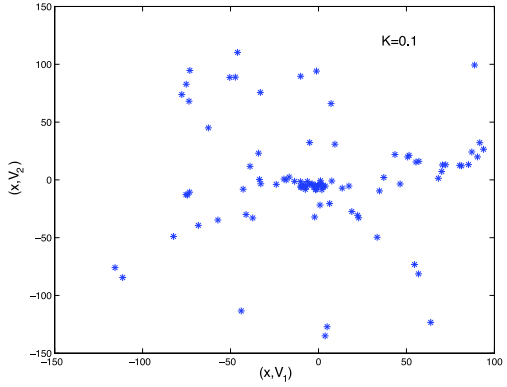

Figure 26. Projection of the dynamics on the first and second eigenvectors for $K = 0.1$ (triangle interaction).

It is only for $K = 0.3$ and 0.7 that the dynamics are almost two dimensional and strongly correlated (Figures 27 to 30).

https://doi.org/10.25088/ComplexSystems.30.1.1

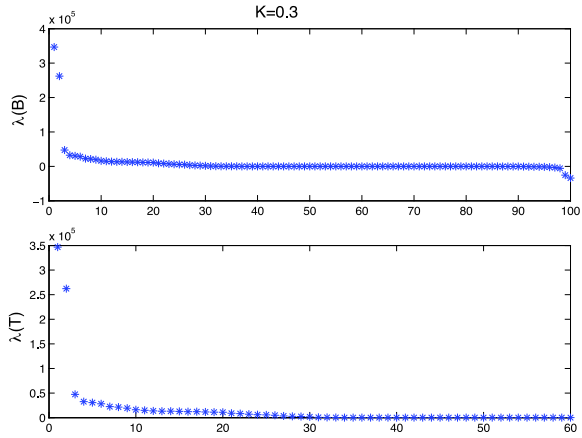

Figure 27. Eigenvalues of the B and T matrices for $K = 0.3$ (triangle interaction).

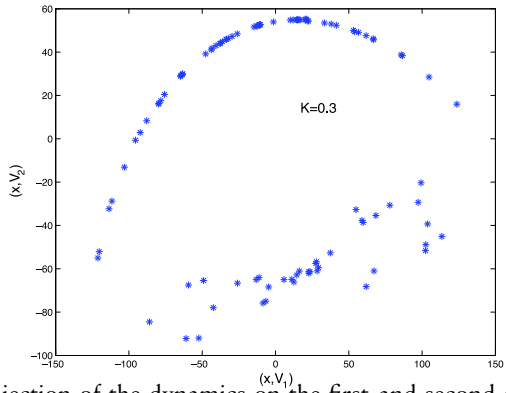

Figure 28. Projection of the dynamics on the first and second eigenvectors for $K = 0.3$ (triangle interaction).

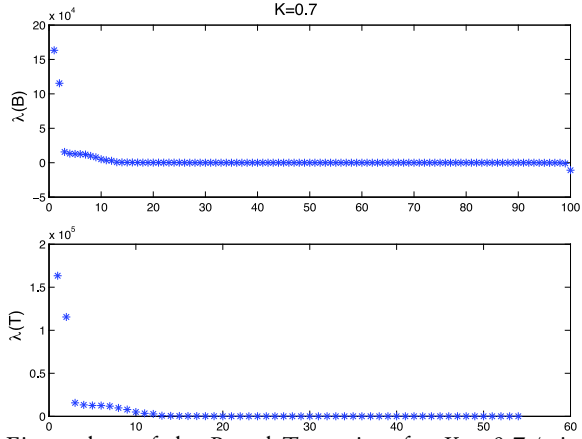

Figure 29. Eigenvalues of the B and T matrices for $K = 0.7$ (triangle interaction).

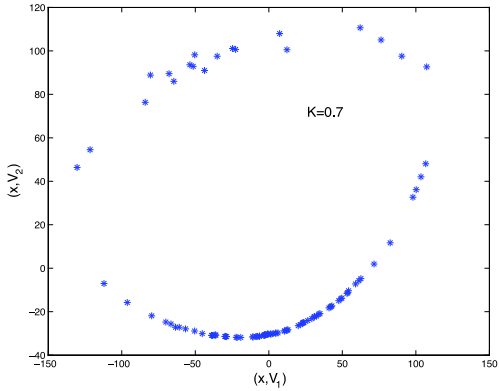

Figure 30. Projection of the dynamics on the first and second eigenvectors for $K = 0.7$ (triangle interaction).

4.2.2 Dynamical Clustering

As before, the dynamical distances and the adjacency matrix are obtained from the coordinate increments. The spectrum of the Laplacian matrix L and the second and third eigenvectors for $K = 0.1$, 0.3 and 0.7 are displayed in Figures 31–33. Some information is obtained from these results, mostly for $K = 0.3$ and 0.7; however, the analysis of the geometry of the dynamics performed in the previous subsection seems to be, in this case, a better way to characterize the correlations.

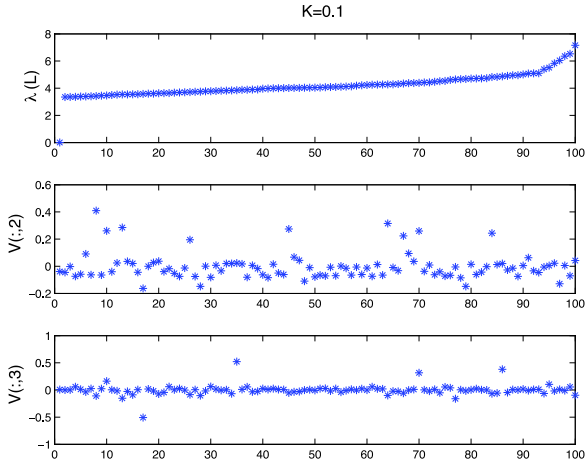

Figure 31. The spectrum of the Laplacian matrix L and the second and third eigenvectors for $K = 0.1$ (triangle interaction).

https://doi.org/10.25088/ComplexSystems.30.1.1

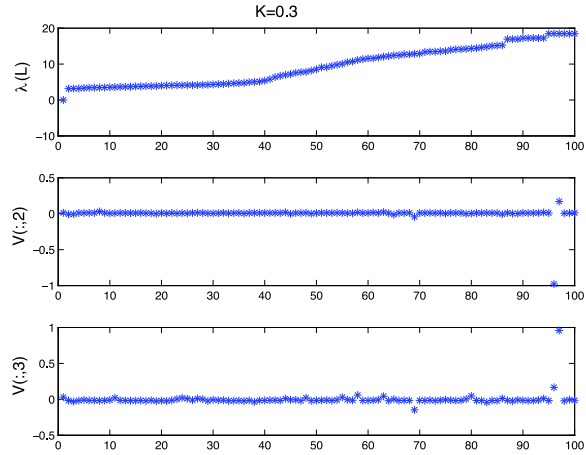

Figure 32. The spectrum of the Laplacian matrix L and the second and third eigenvectors for $K = 0.3$ (triangle interaction).

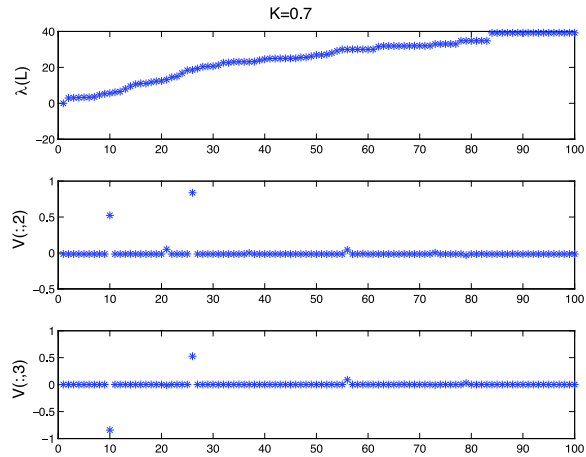

Figure 33. The spectrum of the Laplacian matrix L and the second and third eigenvectors for $K = 0.7$ (triangle interaction).

4.3 A Deterministic "Integrate-and-Fire" Model

Our third example is of a different nature from the previous ones. The dynamic is defined by

$$x_i(t+1) = x_i(t) + s_i + \frac{k}{N-1}\sum_{j\neq i}\theta\left(x_j(t-1) - x_j(t) - 0.4\right) \pmod 1, \tag{26}$$

θ being the function

$$\begin{cases} x > 0 & \theta(x) = 1 \\ x \leq 0 & \theta(x) = 0. \end{cases}$$

The free evolution of each unit is a slow increase during many time steps followed by a jump (Figure 34).

This jump is, by a neuron analogy [7], interpreted as a spike and the interaction with the other units occurs only when they spike. In Figure 35, we display the time evolution of the spiking units obtained for $k = 0$, 0.5, 1.2 and 1.5. The simulations are run from random initial conditions in the unit interval and the s_i are also chosen at random.

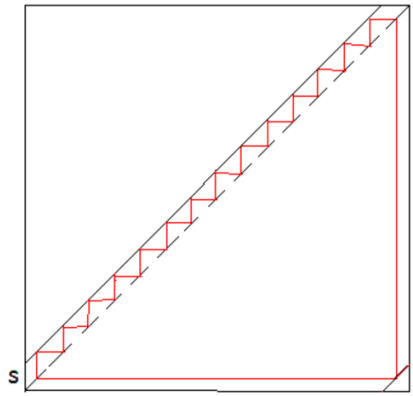

Figure 34. The integrate-and-fire free evolution.

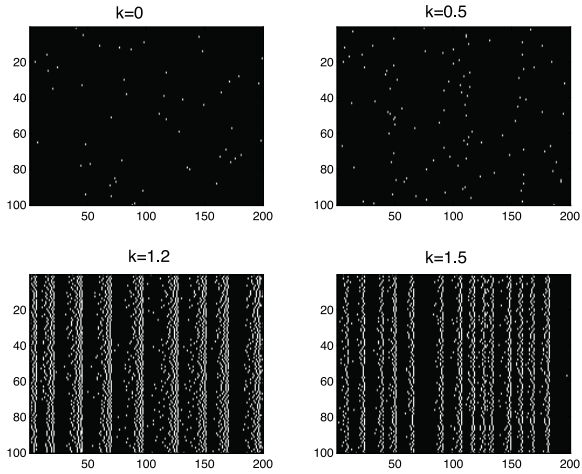

Figure 35. Spiking patterns for different coupling values. 200 time steps, 100 units.

https://doi.org/10.25088/ComplexSystems.30.1.1

As the coupling increases, we see an increase in the spiking rate but not special coordination between the firing times. However, above around $k = 1$ a distinct clustering of the spiking patterns is clearly observed. How these correlations may be characterized will be seen later.

The deterministic integrate-and-fire model is of a different nature as compared to the two previous models. It suggests that in addition to the geometric and clustering methods, which are fairly successful for continuous variable models, other tools should be developed to handle pulsing systems of this type.

To put into evidence the firing patterns, we have displayed the histograms of the firing delays (Figure 36). Here we define the firing delays as the separation in time of each firing from the closest firing in any one of the other units.

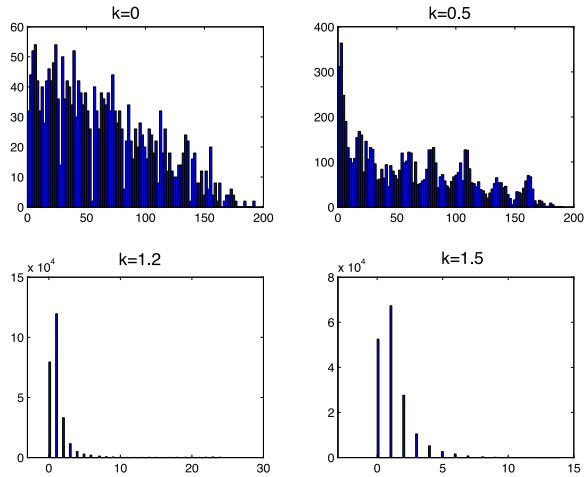

Figure 36. Histograms of the firing delays.

A tendency to organization of the system can be seen in the concentration of the distribution toward smaller delays on passing from $k = 0$ to $k = 0.5$, but it is only only after $k \approx 1$ that the firings organize into a set of well-defined patterns.

From the firing delays, a distance between the units may be defined by the mean of the delays between each pair of units. From the distances, an adjacency matrix was constructed and the spectrum of the Laplacian matrix computed (Figure 37). Some information on the firing clusters is indeed obtained for $k = 1.2$ and 1.5; however, the information provided by the histograms of the firing delays is sharper.

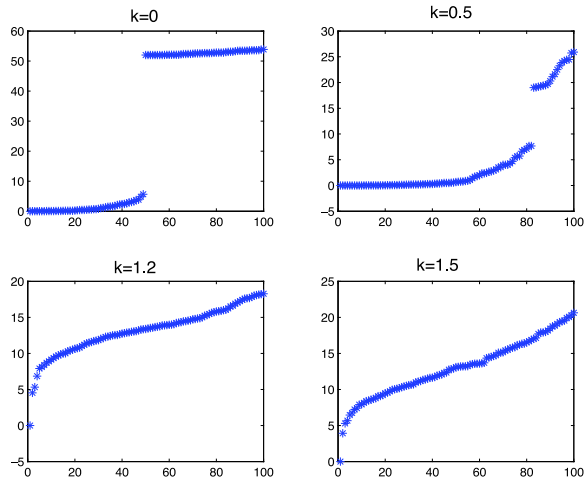

Figure 37. The Laplacian matrix spectrum.

5. Conclusion

From the models analyzed in this paper, it is clear that, in addition to synchronization, other types of strongly correlated behavior emerge in the collective dynamics of interacting systems. What at times has been dismissed as incoherent behavior contains important collective phenomena that enslave the dynamics. Hence, it seemed important to develop tools that might be able to characterize qualitatively and quantitatively the collective correlation effects that emerge before or instead of synchronization. A first step in this direction has been taken in this paper, using geometrical and ergodic techniques.

References

[1] A. Pikovsky, M. Rosenblum and J. Kurths, *Synchronization: A Universal Concept in Nonlinear Sciences*, Cambridge: Cambridge University Press, 2001.

[2] A. Pikovsky and M. Rosenblum, "Dynamics of Globally Coupled Oscillators: Progress and Perspectives," *Chaos: An Interdisciplinary Journal of Nonlinear Science*, **25**(9), 2015 097616. doi:10.1063/1.4922971.

[3] C. W. Wu, *Synchronization in Complex Networks of Nonlinear Dynamical Systems*, New Jersey: World Scientific, 2007.

[4] J. G. Restrepo, E. Ott and B. R. Hunt, "Onset of Synchronization in Large Networks of Coupled Oscillators," *Physical Review E*, **71**(3), 2005 036151. doi:10.1103/PhysRevE.71.036151.

[5] L. Kocarev, ed., *Consensus and Synchronization in Complex Networks*, New York: Springer, 2013.

[6] A. C. J. Luo, *Dynamical System Synchronization*, New York: Springer, 2013.

[7] C. Aguirre, D. Campos, P. Pascual and E. Serrano, "Synchronization Effects Using a Piecewise Linear Map-Based Spiking-Bursting Neuron Model," *Neurocomputing*, **69**(10), 2006 pp. 1116–1119. doi:10.1016/j.neucom.2005.12.056.

[8] A. A. Koronovskii, O. I. Moskalenko, V. I. Ponomarenko, M. D. Prokhorov and A. E. Hramov, "Binary Generalized Synchronization," *Chaos, Solitons and Fractals*, **83**, 2016 pp. 133–139. doi:10.1016/j.chaos.2015.11.045.

[9] L. Glass, "Synchronization and Rhythmic Processes in Physiology," *Nature*, **410**(6825), 2001 pp. 277–284. doi:10.1038/35065745.

[10] D. L. Hayes, S. J. Asirvatham and P. A. Friedman, eds., *Cardiac Pacing, Defibrillation and Resynchronization: A Clinical Approach*, 3rd ed., Chichester, West Sussex, UK: Wiley-Blackwell, 2013.

[11] Z. Lu, K. Klein-Cardeña, S. Lee, T. M. Antonsen, M. Girvan and E. Ott, "Resynchronization of Circadian Oscillators and the East-West Asymmetry of Jet-Lag," *Chaos: An Interdisciplinary Journal of Nonlinear Science*, **26**(9), 2016 094811. doi:10.1063/1.4954275.

[12] A. Schnitzler and J. Gross, "Normal and Pathological Oscillatory Communication in the Brain," *Nature Reviews Neuroscience*, **6**(4), 2005 pp. 285–296. doi:10.1038/nrn1650.

[13] G. J. Ortega, L. M. de la Prida, R. G. Sola and J. Pastor, "Synchronization Clusters of Interictal Activity in the Lateral Temporal Cortex of Epileptic Patients: Intraoperative Electrocorticographic Analysis," *Epilepsia*, **49**(2), 2008 pp. 269–280. doi:10.1111/j.1528-1167.2007.01266.x.

[14] A. A. Ioannides, V. Poghosyan, J. Dammers and M. Streit, "Real-Time Neural Activity and Connectivity in Healthy Individuals and Schizophrenia Patients," *NeuroImage*, **23**(2), 2004 pp. 473–482. doi:10.1016/j.neuroimage.2004.06.023.

[15] A. Sawa and S. H. Snyder, "Schizophrenia: Diverse Approaches to a Complex Disease," *Science*, **296**(5668), 2002 pp. 692–695. doi:10.1126/science.1070532.

[16] P. R. Roelfsema, A. K. Engel, P. König and W. Singer, "Visuomotor Integration Is Associated with Zero Time-Lag Synchronization among Cortical Areas," *Nature*, **385**(6612), 1997 pp. 157–161. doi:10.1038/385157a0.

[17] J.-P. Lachaux, E. Rodriguez, J. Martinerie and F. J. Varela, "Measuring Phase Synchrony in Brain Signals," *Human Brain Mapping*, **8**(4), 1999 pp. 194–208. doi:10.1002/(SICI)1097-0193(1999)8:4%3C194::AID-HBM4%3E3.0.CO;2-C.

[18] M. A. Long, C. E. Landisman and B. W. Connors, "Small Clusters of Electrically Coupled Neurons Generate Synchronous Rhythms in the Thalamic Reticular Nucleus," *The Journal of Neuroscience*, **24**(2), 2004 pp. 341–349. doi:10.1523/JNEUROSCI.3358-03.2004.

[19] J. Buck, "Synchronous Rhythmic Flashing of Fireflies. II," *The Quarterly Review of Biology*, **63**(3), 1988 pp. 265–289. doi:10.1086/415929.

[20] E. Rodriguez, N. George, J.-P. Lachaux, J. Martinerie, B. Renault and F. Varela, "Perception's Shadow: Long-Distance Synchronization of Human Brain Activity," *Nature*, **397**(6718), 1999 pp. 430–433. doi:10.1038/17120.

[21] F. Varela, J.-P. Lachaux, E. Rodriguez and J. Martinerie, "The Brainweb: Phase Synchronization and Large-Scale Integration," *Nature Reviews Neuroscience*, **2**(4), 2001 pp. 229–239. doi:10.1038/35067550.

[22] A. K. Engel and W. Singer, "Temporal Binding and the Neural Correlates of Sensory Awareness," *Trends in Cognitive Sciences*, **5**(1), 2001 pp. 16–25. doi:10.1016/S1364-6613(00)01568-0.

[23] D. Malagarriga, M. A. García-Vellisca, A. E. P. Villa, J. M. Buldú, J. García-Ojalvo and A. J. Pons, "Synchronization-Based Computation through Networks of Coupled Oscillators," *Frontiers in Computational Neuroscience*, **9**, 2015 97. doi:10.3389%2Ffncom.2015.00097.

[24] G. Manzano, F. Galve, G. L. Giorgi, E. Hernández-García and R. Zambrini, "Synchronization, Quantum Correlations and Entanglement in Oscillator Networks," *Scientific Reports*, **3**(1), 2013 1439. doi:10.1038/srep01439.

[25] R. Sevilla-Escoboza, J. M. Buldú, S. Boccaletti, D. Papo, D.-U. Hwang, G. Huerta-Cuellar and R. Gutiérrez, "Experimental Implementation of Maximally Synchronizable Networks," *Physica A: Statistical Mechanics and Its Applications*, **448**, 2016 pp. 113–121. doi:10.1016/j.physa.2015.12.086.

[26] A. Navas, J. A. Villacorta-Atienza, I. Leyva, J. A. Almendral, I. Sendiña-Nadal and S. Boccaletti, "Effective Centrality and Explosive Synchronization in Complex Networks," *Physical Review E*, **92**(6), 2015 062820. doi:10.1103/PhysRevE.92.062820.

[27] M. Golubitsky and I. Stewart, "Rigid Patterns of Synchrony for Equilibria and Periodic Cycles in Network Dynamics," *Chaos: An Interdisciplinary Journal of Nonlinear Science*, **26**(9), 2016 094803. doi:10.1063/1.4953664.

[28] B. Ottino-Löffler and S. H. Strogatz, "Frequency Spirals," *Chaos: An Interdisciplinary Journal of Nonlinear Science*, **26**(9), 2016 094804. doi:10.1063/1.4954038.

[29] P. S. Skardal, D. Taylor and J. Sun, "Optimal Synchronization of Directed Complex Networks," *Chaos: An Interdisciplinary Journal of Nonlinear Science*, **26**(9), 2016 094807. doi:10.1063/1.4954221.

[30] L. Wang and G. Chen, "Synchronization of Multi-agent Systems with Metric-topological Interactions," *Chaos: An Interdisciplinary Journal of Nonlinear Science*, **26**(9), 2016 094809. doi:10.1063/1.4955086.

[31] J. Emenheiser, A. Chapman, M. Pósfai, J. P. Crutchfield, M. Mesbahi and R. M. D'Souza, "Patterns of Patterns of Synchronization: Noise Induced Attractor Switching in Rings of Coupled Nonlinear Oscillators," *Chaos: An Interdisciplinary Journal of Nonlinear Sciences*, **26**(9), 2016 094816. doi:10.1063/1.4960191.

[32] V. V. Makarov, A. A. Koronovskii, V. A. Maksimenko, A. E. Hramov, O. I. Moskalenko, J. M. Buldú and S. Boccaletti, "Emergence of a Multilayer Structure in Adaptive Networks of Phase Oscillators," *Chaos, Solitons and Fractals*, **84**, 2016 pp. 23–30. doi:10.1016/j.chaos.2015.12.022.

[33] R. Sevilla-Escoboza, I. Sendiña-Nadal, I. Leyva, R. Gutiérrez, J. M. Buldú and S. Boccaletti, "Inter-layer Synchronization in Multiplex Networks," arxiv.org/abs/1510.07498.

[34] H. Fujisaka and T. Yamada, "Stability Theory of Synchronized Motion in Coupled-Oscillator Systems," *Progress of Theoretical Physics*, **69**(1), 1983 pp. 32–47. doi:10.1143/PTP.69.32.

[35] L. M. Pecora and T. L. Carroll, "Synchronization in Chaotic Systems," *Physical Review Letters*, **64**(8), 1990 pp. 821–824. doi:10.1103/PhysRevLett.64.821.

[36] R. Vilela Mendes, "Clustering and Synchronization with Positive Lyapunov Exponents," *Physics Letters A*, **257**(3), 1999 pp. 132–138. doi:10.1016/S0375-9601(99)00319-9.

[37] S. Boccaletti, J. Kurths, G. Osipov, D. L. Valladares and C. S. Zhou, "The Synchronization of Chaotic Systems," *Physics Reports*, **366**(1), 2002 pp. 1–101. doi:10.1016/S0370-1573(02)00137-0.

[38] L. M. Pecora and T. L. Carroll, "Synchronization of Chaotic Systems," *Chaos: An Interdisciplinary Journal of Nonlinear Science*, **25**(9), 2015 097611. doi:10.1063/1.4917383.

[39] N. Fujiwara, J. Kurths and A. Díaz-Guilera, "Synchronization of Mobile Chaotic Oscillator Networks," *Chaos: An Interdisciplinary Journal of Nonlinear Science*, **26**(9), 2016 094824. doi:10.1063/1.4962129.

[40] M. Lopez and F. Rodriguez, "Detection Method for Phase Synchronization in a Population of Spiking Neurons," in *Natural and Artificial Models in Computation and Biology (IWINAC 2013)*, Mallorca, Spain, 2013 (J. M. F. Vicente, J. R. Á. Sánchez and F. de la Paz López), Berlin, Heidelberg: Springer-Verlag, 2013 pp. 421–431. doi:10.1007/978-3-642-38637-4_44.

[41] Y. Kuramoto and D. Battogtokh, "Coexistence of Coherence and Incoherence in Nonlocally Coupled Phase Oscillators," *Nonlinear Phenomena in Complex Systems*, **5**(4), 2002 pp. 380–385. www.j-npcs.org/abstracts/vol2002/v5no4/v5no4p380.html.

[42] F. P. Kemeth, S. W. Haugland, L. Schmidt, I. G. Kevrekidis and K. Krischer, "A Classification Scheme for Chimera States," *Chaos: An Interdisciplinary Journal of Nonlinear Science*, **26**(9), 2016 094815. doi:10.1063/1.4959804.

[43] J. D. Hart, K. Bansal, T. E. Murphy and R. Roy, "Experimental Observation of Chimera and Cluster States in a Minimal Globally Coupled Network," *Chaos: An Interdisciplinary Journal of Nonlinear Science*, **26**(9), 2016 094801. doi:10.1063/1.4953662.

[44] D. M. Abrams and S. H. Strogatz, "Chimera States for Coupled Oscillators," *Physical Review Letters*, **93**(17), 2004 174102. doi:10.1103/PhysRevLett.93.174102.

[45] E. A. Martens, C. Bick and M. J. Panaggio, "Chimera States in Two Populations with Heterogeneous Phase-Lag," *Chaos: An Interdisciplinary Journal of Nonlinear Science*, **26**(9), 2016 094819. doi:10.1063/1.4958930.

[46] S. Nkomo, M. R. Tinsley and K. Showalter, "Chimera and Chimera-like States in Populations of Nonlocally Coupled Homogeneous and Heterogeneous Chemical Oscillators," *Chaos: An Interdisciplinary Journal of Nonlinear Science*, **26**(9), 2016 094826. doi:10.1063/1.4962631.

[47] I. Franovic, K. Todorovic, N. Vasovic and N. Buric, "Cluster Synchronization of Spiking Induced by Noise and Interaction Delays in Homogenous Neuronal Ensembles," *Chaos: An Interdisciplinary Journal of Nonlinear Science*, **22**(3), 2012 033147. doi:10.1063/1.4753919.

[48] S. Jalan, A. Kumar, A. Zaikin and J. Kurths, "Interplay of Degree Correlations and Cluster Synchronization," *Physical Review E*, **94**(6), 2016 062202. doi:10.1103/PhysRevE.94.062202.

[49] M. T. Schaub, N. O'Clery, Y. N. Billeh, J.-C. Delvenne, R. Lambiotte and M. Barahona, "Graph Partitions and Cluster Synchronization in Networks of Oscillators," *Chaos: An Interdisciplinary Journal of Nonlinear Science*, **26**(9), 2016 094821. doi:10.1063/1.4961065.

[50] F. Sorrentino and L. Pecora, "Approximate Cluster Synchronization in Networks with Symmetries and Parameter Mismatches," *Chaos: An Interdisciplinary Journal of Nonlinear Science*, **26**(9), 2016 094823. doi:10.1063/1.4961967.

[51] T. Nishikawa and A. E. Motter, "Network-Complement Transitions, Symmetries, and Cluster Synchronization," *Chaos: An Interdisciplinary Journal of Nonlinear Science*, **26**(9), 2016 094818. doi:10.1063/1.4960617.

[52] P. Ji, T. K.DM. Peron, F. A. Rodrigues and J. Kurths, "Analysis of Cluster Explosive Synchronization in Complex Networks," *Physical Review E*, **90**(6), 2014 062810. doi:10.1103/PhysRevE.90.062810.

[53] S. Watanabe and S. H. Strogatz, "Integrability of a Globally Coupled Oscillator Array," *Physical Review Letters*, **70**(16), 1993 pp. 2391–2394. doi:10.1103/PhysRevLett.70.2391.

[54] E. Ott and T. M. Antonsen, "Low Dimensional Behavior of Large Systems of Globally Coupled Oscillators," *Chaos: An Interdisciplinary Journal of Nonlinear Science*, **18**(3), 2008 037113. doi:10.1063/1.2930766.

[55] Y. Kuramoto, *Chemical Oscillations, Waves, and Turbulence*, New York: Springer-Verlag, 1984.

[56] S. H. Strogatz, "From Kuramoto to Crawford: Exploring the Onset of Synchronization in Populations of Coupled Oscillators," *Physica D: Nonlinear Phenomena*, **143**(1), 2000 pp. 1–20. doi:10.1016/S0167-2789(00)00094-4.

[57] J. A. Acebrón, L. L. Bonilla, C. J. Pérez Vicente, F. Ritort and R. Spigler, "The Kuramoto Model: A Simple Paradigm for Synchronization Phenomena," *Review of Modern Physics*, **77**(1), 2005 pp. 137–185. doi:10.1103/RevModPhys.77.137.

[58] R. Vilela Mendes, "Tools for Network Dynamics," *International Journal of Bifurcation and Chaos*, **15**(4), 2005 pp. 1185–1213. doi:10.1142/S0218127405012715.

[59] R. Vilela Mendes, "Ergodic Parameters and Dynamical Complexity," *Chaos: An Interdisciplinary Journal of Nonlinear Science*, **21**(3), 2011 037115. doi:10.1063/1.3634008.

[60] U. von Luxburg, "A Tutorial on Spectral Clustering," *Statistics and Computing*, **17**(4), 2007 pp. 395–416. doi:10.1007/s11222-007-9033-z.

[61] R. Vilela Mendes, "Conditional Exponents, Entropies and a Measure of Dynamical Self-Organization," *Physics Letters A*, **248**(2), 1998 pp. 167–171. doi:10.1016/S0375-9601(98)00604-5.

[62] R. Vilela Mendes, "Characterizing Self-Organization and Coevolution by Ergodic Invariants," *Physica A: Statistical Mechanics and Its Applications*, **276**(3), 2000 pp. 550–571. doi:10.1016/S0378-4371(99)00444-6.